

Stephen R. Herbener* and William R. Cotton
Colorado State University, Fort Collins, Colorado

1. INTRODUCTION

The physical processes that take place in clouds and storms are complex and extremely difficult to measure. Because of this, computer models have been extensively utilized to help researchers gain insight into these processes. One such series of studies, Zhang et. al. (2007), Zhang (2008), Zhang et. al., (2009), utilized the Regional Atmospheric Modeling System (RAMS; Cotton et. al., 2003) to examine the effects of dust acting as CCN on Atlantic tropical cyclones (TC). Early simulations by Zhang et al. (2007) demonstrated a strong response to CCN with greater amounts of CCN decreasing storm intensity. Subsequent simulations (Zhang 2008, Zhang et al. 2009) exhibited a general trend of decreasing storm intensity with increasing CCN but the results were not monotonic. This demonstrates the complexity of interactions of microphysics and dynamics within a TC.

The work to be described is a continuation of the Zhang (2008) study with the purpose of untangling some of the complex microphysical-dynamical interactions in the TC simulations. This study focuses on the investigation of a hypothesis that has been presented to explain the non-monotonic response to enhanced CCN concentration levels. It is proposed that an increase of CCN in the outer rainbands causes reduced collision and coalescence, which results in more supercooled liquid water to be transported aloft which then freezes and enhances convection via enhanced latent heat of freezing. The intensified convection condenses more water which ultimately enhances precipitation in the outer rainbands. Enhanced evaporative cooling from the increased precipitation in the outer rainbands produces stronger and more widespread areal cold pools which block the flow of energy into the storm core and ultimately inhibits the intensification of the TC. However, the amount of suppression of the strength of the TC depends on the timing between the transport of CCN to the outer rainbands and the intensity and lifecycle stage of the outer rainband convection. If the elevated CCN levels are introduced when the outer rainband convection is weak, the transport of significant amounts of supercooled liquid water aloft and the associated dynamic response will not occur.

2. SIMULATION CONFIGURATION AND EXPERIMENTAL DESIGN

It was desired to reproduce the RAMS simulations from Zhang (2008) as closely as possibly so that continuity could be maintained into this work.

The initialization routines (axisymmetric vortex and warm bubble) and RAMS control files used in Zhang (2008) were collected and compiled into RAMS. However, RAMS had undergone improvements in its microphysics routines (cloud droplet modes and riming) since the work of Zhang (2008), and it was preferred to make use of these updates.

A triple two-way interactive nested grid was configured in RAMS using 24km, 6km and 1.5km grid spacing with grid sizes of 1920km, 600km and 300km (grids 1, 2 and 3, respectively). The simulation was set up such that the storm center resided at 15N, 40W on an f-plane based on that location. The time step was set up as 60s, 20s and 10s for grids 1, 2 and 3 respectively. This configuration followed Zhang (2008) with the exception that the grid spacing for the finest grid was reduced from 2km to 1.5km.

The “CCN from boundaries” experiment from Zhang (2008) was selected for this study. This experiment was designed to simulate the action of a TC entering the Saharan Air Layer (SAL) and advecting dust acting as CCN into its interior. Five different magnitudes of CCN concentration were utilized: 100, 500, 1000, 1500, and 2000 cm^{-3} . These CCN concentrations were applied from the surface up to 5km (Figure 1).

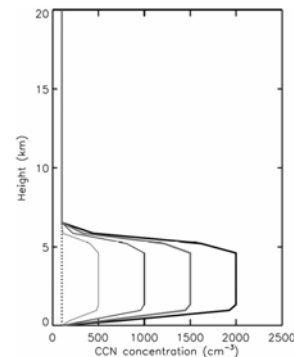


Fig. 2.6. Vertical profiles of the environment CCN with CCN maximum concentration of 100 (dotted line), 500 (thin gray line), 1000 (thin black line), 1500 (thick gray line) and 2000 (thick black line) cm^{-3} .

Figure 1: Vertical profiles of CCN concentration from Zhang (2008)

The TC was allowed to spin up in a single simulation from time zero to 36 hours. Then the experiment was run in a set of five simulations (one for each CCN concentration amount) starting with the results of the initial spin up simulation at 36 hours and continuing to 72 hours. The CCN concentration was set to 100 cm^{-3} for the initial spin up simulation, and then the test CCN concentrations were applied at the onset of the experimental simulations (36 – 72 hrs).

* Corresponding author address: Stephen R. Herbener, Colorado State Univ., Dept. of Atmospheric Science, Fort Collins, CO 80523-1371; e-mail: sherbener@atmos.colostate.edu

In Zhang (2008) grids 1 and 2 were initialized to the CCN concentration being tested in the experimental runs and the resulting CCN was allowed to advect into the inner grid. It was found in early simulation runs that this scheme presented two issues. The first was that the CCN did not seem to advect much beyond the rainband region and the second was that the storm was immediately hit around its entire periphery with the new magnitude of CCN concentration which then persisted throughout the simulation.

In this study the CCN application was modified to present the new magnitude of CCN concentration at only the north boundary of grid 3 in order to simulate the TC entering the SAL from the south. Also, at the onset of the experimental run the CCN concentration was slowly ramped up from the background 100 cc^{-1} level of the initial spin up simulation to the new magnitude being tested.

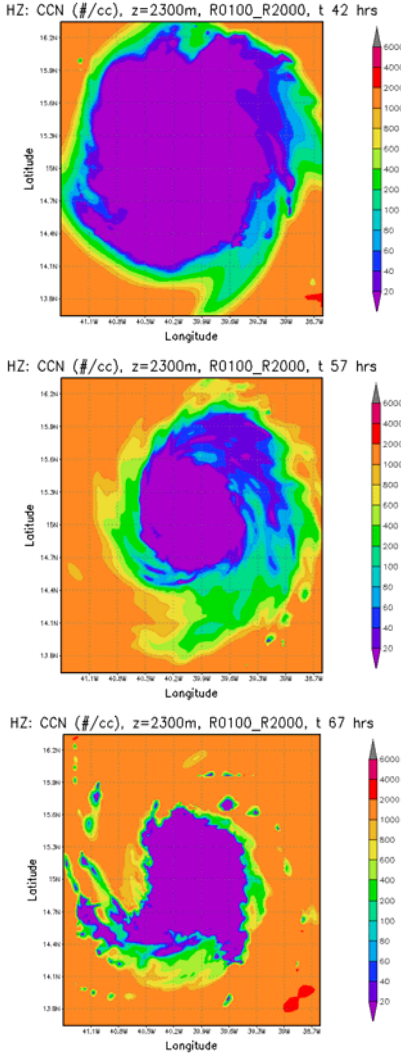


Figure 2: Progression of injected CCN in the R2000 simulation of the HZ experiment. Times are 42hrs (top), 57hrs (middle) and 67hrs (bottom).

Figure 2 and **Figure 3** show the progression of the CCN field at the 2300m level (roughly in the middle of the CCN profile shown in **Figure 1**).

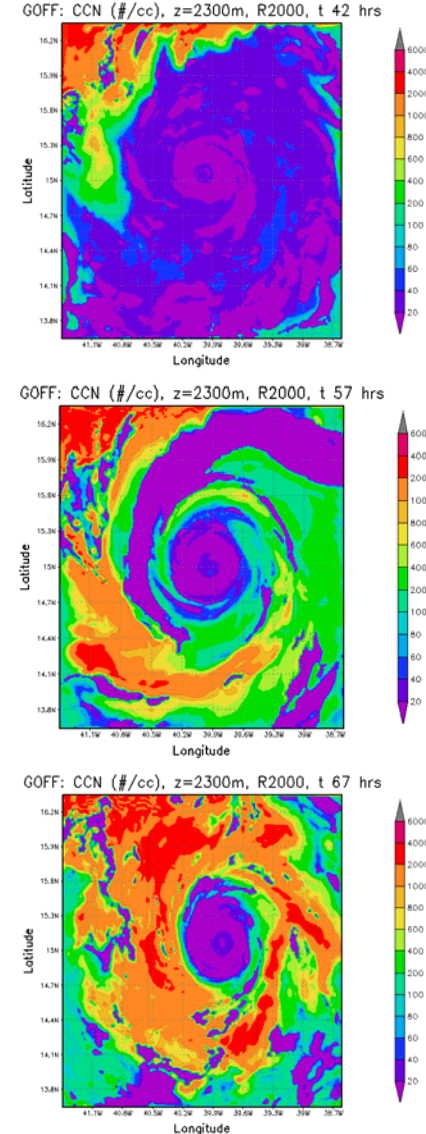


Figure 3: Progression of injected CCN in the R2000 simulation of the GOFF experiment. Times are 42hrs (top), 57hrs (middle) and 67hrs (bottom).

For all simulations a background GCCN and IFN profile (horizontally homogeneous) was applied, and the environment was set using the sounding data from Jordan (1958).

An additional experiment was run using the exact same configuration with the exception that the GCCN concentration was set to an extremely low value (1e-6 cc^{-1}) effectively shutting off the GCCN effects in that simulation.

3. RESULTS

The simulated data from the “CCN from boundaries” experiment from Zhang (2008) was collected and analyzed along with the two experiments from this study. The Zhang (2008) set is labeled with “HZ”, this study’s experiment using the same GCCN concentration as HZ, is labeled “GON”,

and the other experiment using the extremely low GCCN concentration is labeled "GOFF". Within the experiments the CCN concentration is denoted with an "R" followed by the concentration value with the exception in HZ where CLNM represents 100 cc^{-1} .

Figure 4, shows, for the three experiments, the time evolution of a metric designed to reveal the storm intensity which is based on the area coverage of surface winds that are hurricane speed. All data points in the inner grid are compared to the categories of the Saffir-Simpson wind speed scale and then weighted by the hurricane category number (wind speeds less than 33 m/s are given a weight of zero). This was done in an attempt to measure the destructive potential of the storm since some researchers (e.g., Rosenfeld et. al, 2007) have noted that the maximum surface wind speed is not a reliable indicator of the destructive potential of a TC.

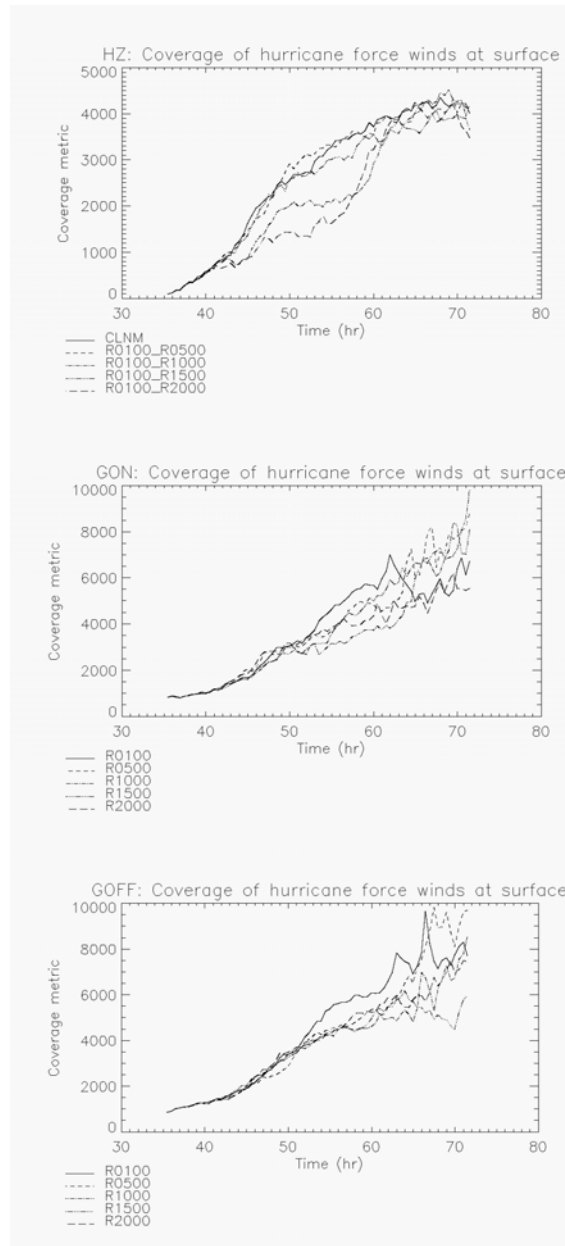


Figure 4: Storm intensity metric for HZ (top), GON (middle) and GOFF (bottom).

The non-monotonic response to the CCN concentration magnitude persists in all three experiments. In HZ it appears that the storms have peaked out around 68hrs, whereas in the GON and GOFF experiments it is not clear if the storms have peaked out by the end of the simulations. Note the significantly larger coverage metric values for GON and GOFF compared to HZ which reflect that GON and GOFF contain physically larger storms which probably evolve more slowly than those of HZ. This presents two issues with GON and GOFF in that it will be necessary to run the simulations beyond 72hrs to know that the maximum intensity has been attained by all the simulated storms; and the grid 3 size of 300km per side is probably not large enough.

Despite these shortcomings, there are some results in GON and GOFF that are of interest. For example there are some indications that the process we are looking for in the hypothesis is taking place and it is more apparent in GOFF than in GON or HZ.

All three experiments progress in a similar fashion up to around 60hrs. The storms with lower concentrations of CCN tend to retain a stronger intensity compared to those with higher CCN concentrations. However, by 67hrs this distinction diminishes greatly in the HZ experiment and vanishes in the GON experiment; yet in the GOFF experiment there still remains a fairly clear difference between the storms with low CCN amounts versus the storms with high CCN amounts.

The change that takes place in the progression of the three experiments at 67hrs makes this an interesting point to examine further. The R1500 storm in all three experiments tends to remain fairly steady without any large jumps or oscillations in intensity. Furthermore, R1500 steadily increases in intensity on past 67hrs in the HZ and GON experiments whereas it turns the corner and diminishes in the GOFF experiment. These results make R1500 a good representative for closer examination. Since HZ and GON have similar behavior for the R1500 storm, only the GON data will be shown.

Figure 5 shows contour frequency by altitude diagrams (CFAD, see Yuter and Houze 1995 for more details) of the vertical velocity in the outer rainband region for the R1500 simulations for both GON and GOFF at time 67hrs.

Note in **Figure 5** the lack of low level downdrafts in the outer rainbands for the GON experiment which indicates the likelihood that lower level cooling is not taking place. This allows the supply of warm moist air from the ocean surface to proceed into the core of the storm resulting in the storm retaining strong intensity. The GOFF experiment also contains much more strong updrafts suggesting more of its storm area contains convective activity in the outer rainbands.

Figure 6 shows the azimuthally averaged temperature fields for both the GON and GOFF R1500 simulations at 67hrs. The temperature data was conditionally selected in the regions that had significant vertical velocity (absolute value of $w >=$

1.0 m/s) anywhere in the column where the temperature point existed. The greater lower level cooling is apparent in the GOFF simulation as expected.

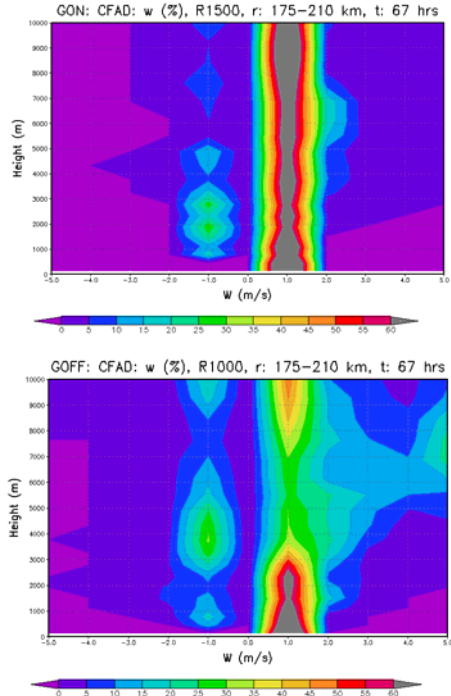


Figure 5: Vertical velocity (CFAD) in the outer rainband region (radius 175-210 km) at 67 hrs for the GON (top) and GOFF (bottom) R1500 simulations.

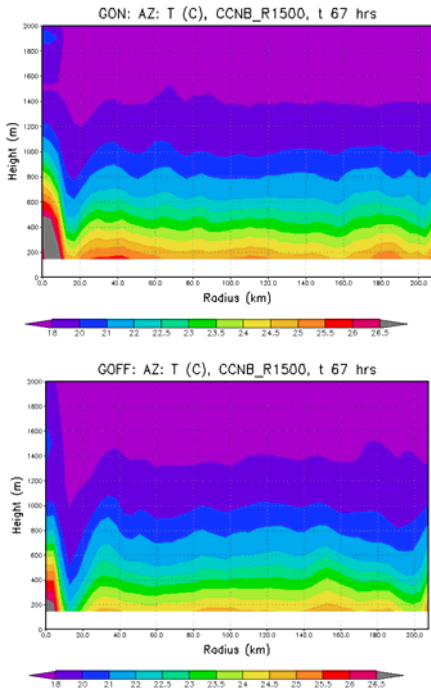
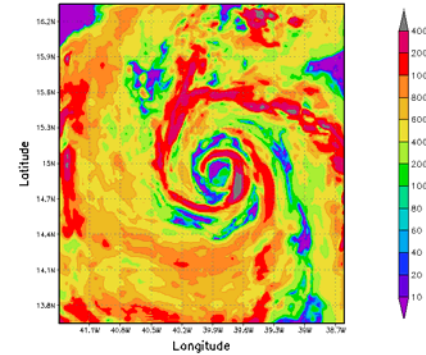


Figure 6: Azimuthally averaged temperature (°C) at 67 hrs in the GON (top) and GOFF (bottom) R1500 simulations.

GON: Supercooled LWP (g/m2), R1500, t 67 hrs**



GOFF: Supercooled LWP (g/m2), R1500, t 67 hrs**

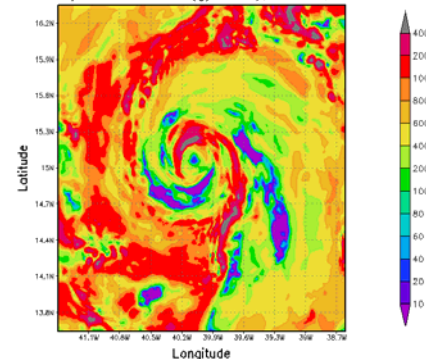
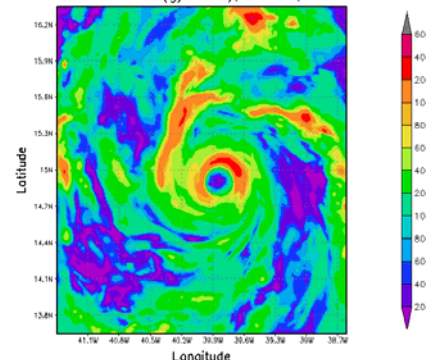


Figure 7: Supercooled liquid water path at 67 hrs in the GON (top) and GOFF (bottom) R1500 simulations.

GON: Warm LWP (g/m2), R1500, t 67 hrs**



GOFF: Warm LWP (g/m2), R1500, t 67 hrs**

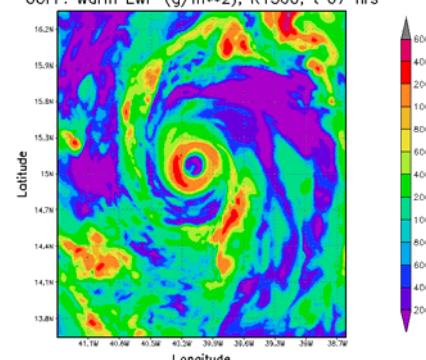


Figure 8: Warm liquid water path at 67 hrs in the GON (top) and GOFF (bottom) R1500 simulations.

Figure 7 displays the liquid water path (LWP) for both the GON and GOFF R1500 experiments at 67hrs. Supercooled liquid water was conditionally selected for these plots. Note that there are significantly higher amounts of supercooled water in the outer rainband region. **Figure 8** is the same as **Figure 7** except that for this plot the liquid water was conditionally selected where the temperature was above freezing. Note that GOFF contains larger regions in the outer rainbands that lack warm liquid water. This suggests that the warm rain processes are suppressed in the outer rainband region more so for GOFF than GON.

4. DISCUSSION AND SUMMARY

The data presented so far are consistent with the notion that higher concentrations of CCN in the rainbands cause elevated amounts of supercooled liquid water aloft. This activity then enhances convection and ultimately low level evaporative cooling in the rainband region which then cuts off the energy source to the storm resulting in a reduction of storm intensity. The question remaining is why did the GON and GOFF experiments diverge when they both were presented with the same concentration level of CCN?

It seems that in the GON experiment since it had the same concentration of CCN as GOFF that it should have also enhanced the supercooled liquid water content via suppression of collision and coalescence. However, GON had a significantly higher level of GCCN which would tend to form large droplets in the region where the CCN was forming small droplets. This situation is quite different than that of GOFF (narrow droplet size distribution with small droplet size). In GON there existed many small droplets mixed with a few large droplets; a situation that would tend to *enhance* collision and coalescence resulting in reduced supercooled liquid water and increased warm rain.

In a real TC situation there would be a mix of GCCN levels. The primary source of GCCN over the ocean is sea spray which evaporates leaving salt particles in the air (Andrea and Rosenfeld, 2008, O'Dowd et. al., 1997). The wind speed needs to be around 9 m/s in order to initiate the production of sea spray GCCN and greater than 17m/s to produce large amounts of GCCN (O'Dowd et. al., 1997). The wind speeds in the outer rainbands would be slow enough as to not generate much GCCN (sea spray), but the wind speeds in the interior of the storm would be sufficiently strong to generate significant amounts of GCCN. Therefore, in a real TC it would be expected to have high levels of GCCN in the interior of the storm and low levels of GCCN in the outer rainband region. Unfortunately, neither of GON nor GOFF simulated this situation.

Work is in progress to incorporate a sea spray GCCN source model into RAMS. This addition will allow a simulation which models the GCCN field in a TC more accurately.

The idea that the impacts on the TC can be quite different when GCCN and CCN interact together versus when CCN acts alone can help explain some

of the non-monotonic behavior of the response to different CCN concentration levels. This can be seen to some degree in the storm intensity plots. However, the removal of GCCN did not result in a monotonic response in the GOFF experiment.

It is still possible that the main hypothesis of this study is also a factor in the non-monotonic response. The data appear to support the microphysical-dynamical interaction piece of the hypothesis, but the timing aspect has not been worked out yet.

The next steps for this research will be to rerun the experiment using the new sea spray GCCN source model in RAMS, resolve the issues with the grid 3 size and simulation end time, and to test whether or not the timing of CCN introduction in relation to the rainband convection development is a factor in the resulting storm intensity.

5. ACKNOWLEDGEMENTS

This research was funded by DHS/NOAA under contract NA17RJ1228.

6. REFERENCES

Andrea, M. O., D. Rosenfeld, 2008: Aerosol-cloud-precipitation interactions. Part 1. The nature and sources of cloud-active aerosols, *Earth-Sci. Rev.*, **89**, 13-41.

Cotton, W. R., R. A. Pielke, Sr., R. L. Walko, G. E. Liston, C. J. Tremback, H. Jiang, R. L. McAnelly, J. Y. Harrington, M. E. Nicholls, G. G. Carrio, and J. P. McFadden, 2003: RAMS 2001: Current status and future directions. *Meteor. Atmos. Phys.*, **82**, 5-29.

Jordan, C. L., 1958: Mean soundings for the West Indies area. *J. Meteor.*, **15**, 91-97.

O'Dowd, C.D., M.E. Smith, I.E. Consterdine and J.A. Lowe, 1997: Marine aerosol, sea-salt, and the marine sulphur cycle: A short review. *Atmos. Environ.*, **31**, 73-80.

Rosenfeld D., A. Khain, B. Lynn, and W. L. Woodley, 2007: Simulation of hurricane response to suppression of warm rain by sub-micron aerosols, *Atmos. Chem. Phys.*, **7**, 3411-3424.

Yuter, S.E., and R. A. Houze, 1995: Three-Dimensional Kinematic and Microphysical Evolution of Florida Cumulonimbus. Part II: Frequency Distributions of Vertical Velocity, Reflectivity, and Differential Reflectivity, *Mon. Wea. Rev.*, **123**, 1941-1963

Zhang, H. (2008), Impact of Saharan dust as CCN on the evolution of an idealized tropical cyclone, *PhD dissertation, University of Illinois*

Zhang, H., G. M. McFarquhar, S. M. Saleeby, and W. R. Cotton (2007): Impacts of Saharan dust as CCN on the evolution of an idealized tropical cyclone, *Geophys. Res. Lett.*, **34**, L14812, doi:10.1029/2007GL029876.

Zhang, H., G. M. McFarquhar, W. R. Cotton, and Y. Deng (2009): Direct and indirect impacts of Saharan dust acting as cloud condensation nuclei on tropical cyclone eyewall development, *Geophys. Res. Lett.*, **36**, L06802, doi:10.1029/2009GL037276.